

A unified method for 2-D and 3-D refraction statics

M. Turhan Taner*, Donald E. Wagner[‡], Edip Baysal*, and Lee Lu**

ABSTRACT

Most of the seismic data processing procedures are divided into 2-D, 2.5-D, crooked lines or 3-D versions dictated by the differences in the shot and receiver configurations. In this paper, we introduce a tomographic approach that overcomes these geometrical difficulties and provides stable statics solutions from picked first-break times. We also show that the first-break picks contain both the short and the long wavelength surface statics. The solutions are obtained by solving a set of generalized surface-consistent delay-time equations using the method of weighted least squares and conjugate gradient. While iterating, each first-break pick is evaluated to ensure its consistency with the least-squares solution. Based on consistency, we weight the traveltime picks and use them in the next iteration. These weights also serve as an indicator of anomalous picks to the user.

We show that long wavelength solutions leave large residual errors in the least-squares solutions. We also use the expected length of the Fresnel zone to differentiate between short and long wavelength static solutions. After removing the influence of long wavelength statics, we apply short wavelength statics to reduce the residual errors further.

We demonstrate the validity of our unified method by applying it to actual data examples. The removal of both long and short wavelength statics improves the initial data set that produces a more consistent set of velocities and leaves only the short wavelength residual reflection statics, which are generally less than quarter wavelet period delays. This removes the most probable cause of the leg jump contamination and poor velocity estimates from the residual statics computations, especially from the 3-D data.

INTRODUCTION

Interpretation of refracted seismic data precedes that of the reflected data in early applications. Thornburgh and Ansel published their papers in 1930. Hagedoorn (1959) gave a modified graphical solution of the Ansel and Thornburgh method. A number of refraction papers edited by Musgrave (1967) were published by SEG. Later, Palmer (1980) published the generalization of the reciprocal method. Hampson and Russell (1984) and Schneider and Kuo (1985) gave solutions based on tracing rays through refractor models. The tomographic computations were introduced initially for wellbore to wellbore measurements to determine the velocity and image structure between wells. Chun and Jacewitz (1980 and 1981) discussed the content of the first arrivals and presented a surface consistent solution of refraction statics by the formation of time surfaces. They also indicated that large error distributions often remained after solutions have been obtained. These deviations attracted our attention and led us to classify them as surface generated

delays. Farrell and Euwema (1984) gave a least-squares solution that computes refractor geometries from first-break picks. Hampson and Russell (1984) presented a generalized linear inversion scheme to determine the refractor geometry from picked first breaks. In this least-squares method, Hampson and Russell achieve convergence by minimizing the difference of traveltimes of rays traced from the computed model versus the actual first-break pick times. They constrain the lateral geometrical variation of both the layer thickness and velocities to minimize the effects of the short wavelength undulations in the picked times. The first paper that applied tomography to refraction statics was given by Chon and Dillon (1986). They presented Gauss-Seidel iterative methods for computation of statics by the delay time method. This method was described initially by Barry (1967), who pointed out that the delay time method (Gardner, 1939) can be generalized to arrive at a solution for long wavelength 2-D and 3-D refraction statics.

This generalization becomes a tomography problem in which the refractor velocities and shot and receiver related delay

*Rock Solid Images, www.rocksolidimages.com, 2600 South Gessner Suite 650 Houston, Texas 77063, - mt.taner@rocksolidimages.com

‡AMOCO, Box 800, Denver, CO 80201. E-mail: dwagner@den.amoco.com.

**Leading Seis Inc., 3707 Ingold Street, Houston, TX 77085. E-mail: leelu@hal-pc.org.

© 1998 Society of Exploration Geophysicists. All rights reserved.

times are computed from the first-break times with arbitrary shot-receiver positions, azimuths, and offsets. Kirchheimer (1988) and Taner et al. (1988) discuss the long wavelength refraction statics solutions.

Unlike the averaging approach to tomographic computation of statics used by Chon and Dillon (1986) and others, we use a weighted least-squares approach in conjunction with the conjugate-gradient algorithm (Wang and Treitel, 1973; Koehler and Taner, 1985) to solve the large set of equations arising from the tomographic problem. The method is general enough that 2-D refraction lines, wide-line profiles, and crooked or slalom lines all become special cases of the 3-D problem. The weighted least-squares method is chosen to minimize the contaminating effects of unreliable first breaks. Although the computational procedure assumes that the input data are correct, in reality, we must provide for mispicks and use procedures to minimize their effects.

SURFACE MODEL

Most papers presenting refraction statics computations assume a very simplified model of the near surface. In a recent paper (Docherty, 1992), the layer from surface to the first refractor is defined as the weathered layer. This paper considers the variation of thickness and velocity of this near surface layer and proposes a tomographic solution. Docherty observes that in areas of rapid surface elevation changes, the velocities are determined more accurately while in other areas accuracy is not maintained. This can be explained easily by the Eikonal relationship at the surface. The velocity and arrival-angle ambiguity can be solved only by independent observations of the upward traveling wavefield along x - and z -axes. Since refracted waves cannot resolve this overburden velocity/propagation exit angle ambiguity, most papers assume that the surface velocity is known or determined from other observations. The near-surface depth models are computed from picked first-break times and from these overburden velocities. However, the short wavelength undulations of the pick times cannot be accurately modeled by ray tracing. Furthermore, these short wavelength undulations are not generated by the refracting interface because their Fresnel zone (Sheriff, 1991) at the surface will be large. As we show schematically in Figure 1, waves generated from a small feature on the refractor will cover a wider area when they arrive at the surface, hence

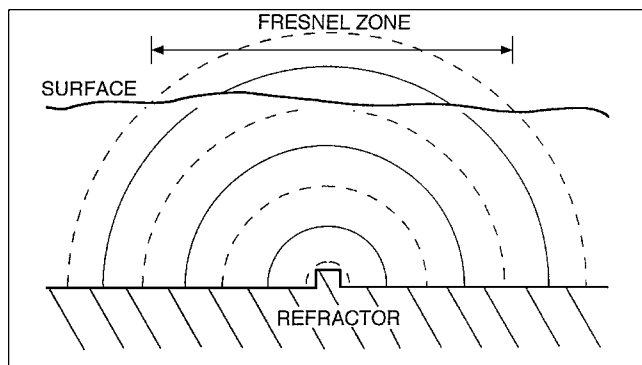


FIG. 1. Schematic diagram of waves and Fresnel zone from a small feature on the refractor.

they will be indistinguishable from longer features. Waves arriving from small river channels or washouts, like the one depicted in Figure 2, will also diffract and since we pick only the first arrivals, some of the short wavelength details will be lost. If we wish to recover these details, we must use seismic imaging techniques, rather than picked first-break times (Taner et al., 1992).

Our primary objective in this work is to determine the long wavelength statics caused by the spatial variation of refractor geometries and the overburden velocities. Therefore, long wavelength solutions of refractor geometry without the short wavelength details would be sufficient for our purposes. We cannot determine directly the interval (overburden) velocity of the layer above the refractors from the first-break times. The most convenient procedure is to compute normal moveout (NMO) velocities from the reflected waves coming from the refractors and estimate interval velocities. Estimating overburden velocities from direct arrivals generally is risky, since most direct arrivals are actually refracted arrivals. One of the more convenient but heuristic methods is to try several velocities and generate corresponding stacked sections, then choose the overburden velocity that produces the least undulating reflectors. This approach was first presented by GeoSource in their Refraction Statics pamphlet in the early 1980s.

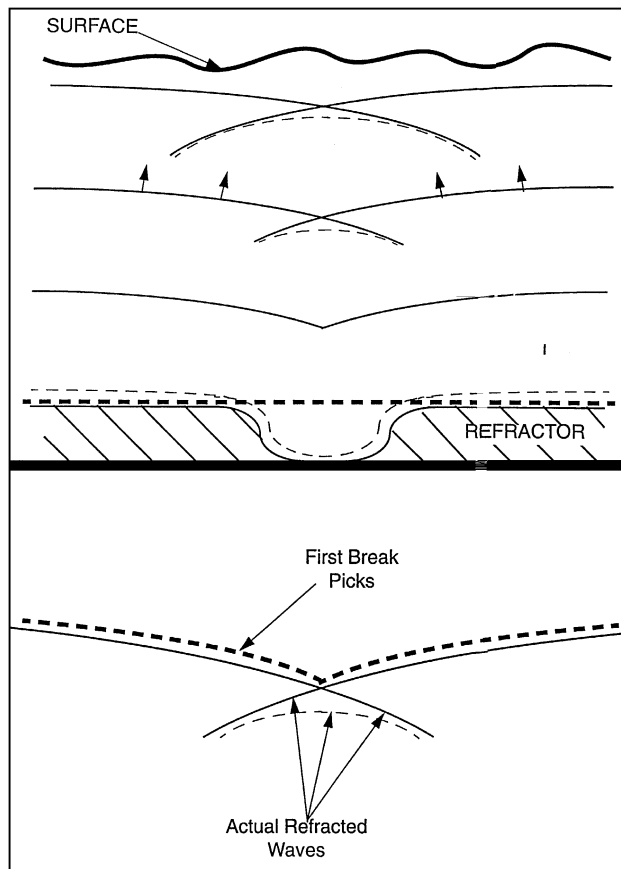


FIG. 2. Waves arriving from a small river channel on the refractor.

LONG AND SHORT WAVELENGTH STATICS

Wave propagation through the earth is controlled directly by the structure of the velocity field. We measure the waves arriving at the surface by receiver arrays at some predesigned intervals. Discretely sampled continuous wavefield can be re-constructed up to some maximum frequency and minimum wavelength. Therefore we cannot account for the perturbation of the wavefield shorter than some wavelength. Sampling theory suggest that we need at least four samples per (shortest) wavelength to be able to estimate the amplitude and the phase of the propagating wavefield. Furthermore, our ability to define the velocity structure of the earth is also limited, on the order of several hundreds of meters. Therefore, the combination of the limited definition of the velocities and discrete sampling of the wavefield will confine us to define the propagation with longer wavelengths. We will call all of the disturbances below this limit “the short wavelength statics.” Dimensionally, they will be on the order of four to eight times the receiver interval. All of the longer wavelength near-surface effects will be classified as the long wavelength statics. Because of the nature of the short wavelength statics, we claim that, they are generated near the surface, basically effecting only the upward travelling waves.

PRESENT WORK

In our work we divide the near surface into two zones. The first zone, the weathered layer at the surface, consists of very low velocity material. Its surface and base are assumed to have any type of undulations including the short wavelength undulations as shown in Figure 3. Since we measure the surface elevations, both its thickness and velocity are unknown. The layer below the weathered layer is more consolidated and it continues more or less uniformly down to the refracting layer. We assume this layer and the top of the refracting layer vary smoothly in the spatial direction, both in thickness and velocity. This model fits with our observations and as we will show later it also fits with our computational model. As depicted in Figure 4, the observed first-break arrival times contain both short and long wavelength undulations. Because of the length of the Fresnel zone of waves arriving from the refracting surface (as shown on Figure 1) only the longer wavelength undulations of the first-break times can be attributed to the refracted first arrivals. Therefore, the short wavelength perturbations must be generated in the surface weathered layer. We assign the

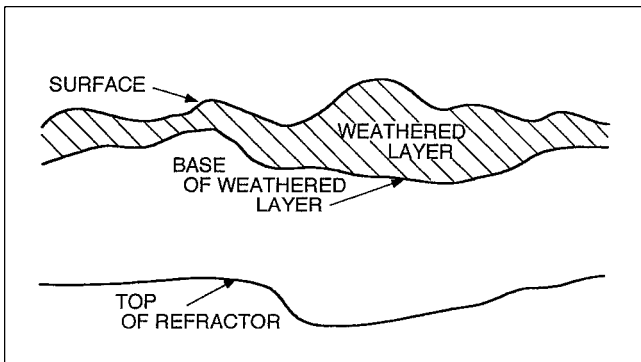


FIG. 3. The near-surface model.

long wavelength portion of the first-break pick times to the refractor computation and the short wavelength portion to the near-surface statics computation. The general model will be defined as

$$t(n, m) = S(n) + R(m) + \sum [\sigma(k) \cdot \Delta(k)] + s(n) + r(m), \quad (1)$$

where

$t(n, m)$ = picked first-break time for n th shot and m th receiver location.

$S(n)$ = delay time at n th shot location, corresponding to the long wavelength source statics.

$R(m)$ = delay time at m th receiver location, corresponding to the long wavelength receiver statics.

$\sigma(k)$ = slowness at k th cell located along the horizontal path between n th and m th surface stations,

$\Delta(k)$ = subpath length in the k th cell of the path between n th and m th surface stations. The sum of the product of subpath length and slowness will give the traveltime along the refractor between the shot and the receiver,

$s(n)$ = short wavelength surface static at the n th shot position n .

$r(m)$ = short wavelength receiver static at the m th receiver position m .

The components of the traveltime are shown on Figure 5. We are also assuming that the picked traveltimes are corrected to the surface by adding the uphole time to the picked first-break time. In the case of deep hole dynamite, we may not have a residual surface shot static component. However, experience has shown that the uphole times usually contain timing errors. Thus, we leave the shot residual statics as one of the unknowns to detect or guard against errors in uphole times.

INITIAL CONSIDERATIONS

Data used for refraction statics computation are the first-break picks. These picks, however, contain a number of errors originating from several factors. One of the most common errors is erroneous pick time. This could occur for several reasons:

- 1) A simple leg-jump, usually one or two wavelengths away from the good pick position,
- 2) A leg-jump caused by following the wrong refractor at a branch point,
- 3) Leg jump caused by the uncertainty of the first break of poorly correlated vibratory data,
- 4) Picking noise caused by the changing first-break characteristics or wavelet shapes,
- 5) Picking time error due to the errors in uphole times for dynamite data,
- 6) Changing wavelet shapes from shot to shot.

Of the data problems, the uphole times and leg jumps are the leading timing errors.

NATURE OF FIRST-BREAK WAVELETS

We assume that first breaks usually are the arrivals from shallow refractors. The refracted arrivals caused by their angle of emergence will have a phase rotation difference from the reflected waves beyond the critical angle. They also have a dispersive nature, therefore the rotation angle changes over distance. For accurate picking, it would be ideal if the picks could be made over shorter offset ranges. Their shapes also depend on the source wavelet shape, which changes from shot to shot on land records. This change leads to shot to shot pick time errors. To alleviate this, first-break wavelet shaping, similar to the seismic signature estimation and shaping, is performed (See Robinson and Osman, 1996). This forces first-break wavelets to have a uniform shape, hence the picks will occur at the same position of the wavelets. Vibratory data generally have the poorest first breaks. Wavelet shaping the first breaks to a minimum phase wavelet with a bandwidth providing the least precursor reverberation is a good procedure for successful automatic and interactive picking.

UNIFIED METHOD FOR STATICS COMPUTATION FROM FIRST-BREAK PICK TIMES

We start with the classical delay time equation (Thornburgh, 1930; Ansel, 1930; Hagedoorn, 1959) and develop an algorithm for estimating delay times for refractors, residual statics from near-surface anomalies and refractor velocities from picked first-arrival times. From these estimates of residual statics, delay times, and refractor velocities, we compute a set of surface consistent static corrections for each source and receiver location. Care is taken to cast the problem in a X, Y, Z coordinate system for application to 3-D data, wide-line profiles, and crooked lines, as well as conventional 2-D linear profiles.

COMPUTATIONAL STEPS

To ensure the consistency of pick times, we shape the first-break zones to a uniform wavelet shape. The optimum shape is a minimum-phase wavelet with the same bandwidth as the first-break wavelet. This is very important particularly for vibratory records with reverberant precursors. Uniformly shaped first-break wavelets produce less picking noise. Details of automatic picking using artificial intelligence techniques are given elsewhere (Veezhinathan, 1990; Veezhinathan et al., 1991; Taner, 1988). Here we assume the first breaks of shot records are picked properly. By this we mean that the picked times are consistent and have a minimum number of errors. These errors are assumed to be scattered throughout the data and are not congested in a particular area. We will address the pick errors further in our computation. The refraction statics computational steps include both the long and short wavelength solutions as follows.

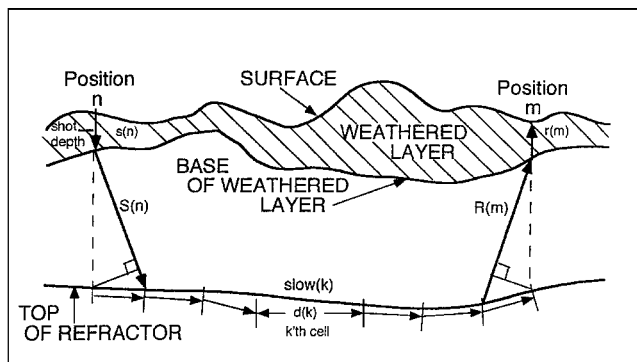


FIG. 5. The travel path in the near surface model.

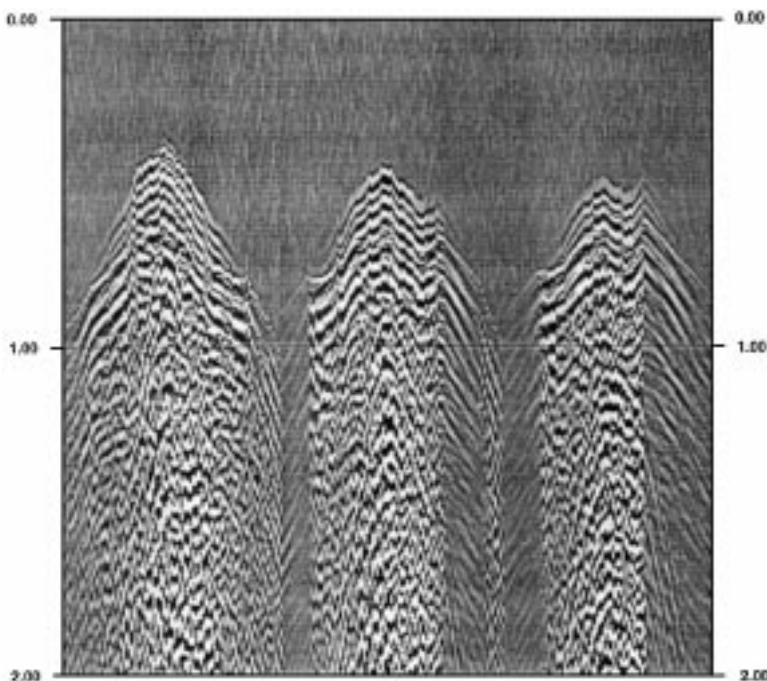


FIG. 4. A seismic record depicting the first-break times with both short and long wavelength undulations.

LONG WAVELENGTH SOLUTION

If the source is dynamite, then we modify the traveltime, in equation (1), by adding the uphole times $up(n)$ to the picked first-break time,

$$T(n, m) = t(n, m) + up(n). \quad (2)$$

Since near-surface elevation and the surface statics affect the refracted arrival times, we compute a smooth (consistent with the wavelength separation of the short and long wavelength statics) near-surface elevation $\tilde{z}(n)$ and an elevation correction between the smooth surface and the actual surface elevation $z(n)$. The pick times to the smooth surface are then corrected,

$$\tilde{t}(n, m) = T(n, m) - elcor(n) - elcor(m), \quad (3)$$

where $\tilde{t}(n, m)$ is the modified pick times and $elcor(n)$ is the elevation correction at n th surface position. The elevation correction at a location (n) is defined by

$$elcor(n) = (z(n) - \tilde{z}(n))/v(\text{weathering}). \quad (4)$$

The more accurate surface weathering velocity $v(\text{weathering})$ may be determined experimentally by applying elevation corrections with different velocities and choosing the one producing the smoothest first-break arrival times.

We assume this corrected time now principally contains the sum of the delay times at shot and receiver positions and the traveltime along the refractor in between. We compute the refractor slownesses and the delay times by minimizing the traveltime error equations

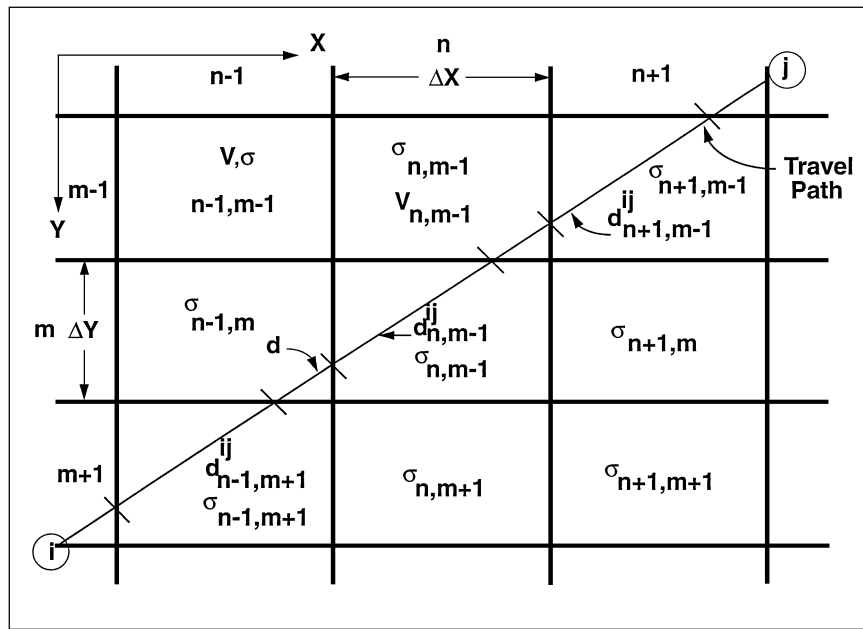
$$\varepsilon = \sum_n \sum_m \left[w(n, m) \cdot \left[\tilde{t}(n, m) - S(n) - R(m) - \sum_k (\sigma(k) \cdot \Delta(k)) \right] \right]^2, \quad (5)$$

where $w(n, m)$ are the weights of each pick time. These are initially set equal to 1. In a computational procedure, we stop the computation after a preset number of iterations (say 15 to 20) and check the error for each pick. We determine the mean error and the standard deviation. This gives an idea of the amount of errors in the pick times. Based on the error statistics we assign weights to each pick proportional to its error range. If each error is given by " $\varepsilon(n, m)$," and the threshold error value is given as some percentage of the standard deviation " $\bar{\varepsilon}$," then we compute the weights by the sigmoidal function,

$$w(n, m) = 1.0/[1.0 + (\varepsilon(n, m)/\bar{\varepsilon})^p], \quad (6)$$

where p is an even constant. This will range from 2 to 8. Smaller values will be more tolerant than the larger values. Weights given by the above expression vary between 0. and 1.0. It will be equal to 1/2 for errors equal to the chosen threshold. In the following iterations, we locate the picks with large errors and smaller weights to isolate and reduce their effects on the final solution.

For crooked lines or for 3-D geometry, we modify equation (1) to handle travelpaths across an areal grid. This 3-D generalization becomes a tomography problem in which refractor velocities are computed from first-arrival traveltimes received at arbitrary shot-receiver azimuths and offsets. The generalized traveltime/path model for 3-D geometry is shown in Figure 6. In this 3-D case, we subdivide the refractor surface into regular rectangular bins (cells), with a bin size of ΔX and



Generalized travel path/time model for 3-D geometry.

FIG. 6. The generalized travel path across a real grid for a 3-D geometry.

Unified Refraction Statics

ΔY in the X and Y directions, respectively. To each bin, we assign a velocity and denote East-West bin indices by n and north-south bin indices by m . Then, the slowness of the refractor in bin n, m is given by σ_{nm} or $(1/V_{nm})$. The path from source location i to receiver location j is to be divided into subpaths d_{ij} . Each subpath represents the individual path across a single bin. Using superscripts to represent the source and receiver positions and subscripts to represent the bin coordinates of the component segments, the delay time equation for the 3-D case becomes

$$T_{ij} = S_i + R_j + \sum_i^j d_{nm}^{ij} \cdot \sigma_{nm}. \quad (7)$$

Our objective is to solve equation (7) for S , R , and σ . We propose an iterative approach that breaks the problem into two subproblems: one solves for the slowness σ , and the other solves for the delay times S and R , as shown in the two steps below.

- 1) Assume S_i and R_j are known and solve for σ values.
- 2) Substitute values of σ into equation (7) and solve for S_i and R_j .

To solve for slowness σ in step (1), modify the picked times to

$$T'_{ij} = T_{ij} - S_i - R_j. \quad (8)$$

Equation (8) multiplied by the corresponding weights is written in the matrix form as $\mathbf{D}\sigma = T'$. To minimize the least-square errors, in the conventional way, we determine and solve the following equation

$$\mathbf{D}'\mathbf{D}\sigma = \mathbf{D}'T', \quad (9)$$

where \mathbf{D}' is the transpose of matrix \mathbf{D} . The dimensions of \mathbf{D} consist of the number of picked times by the number of bins in the area. The conventional solution to this very large matrix equation is impractical. We solve equation (9) by the conjugate gradient method (Wang and Treitel, 1973; Koehler and Taner, 1985). The advantage of this method is its robustness, speed of convergence, and its immunity to various instabilities inherent in surface consistent equations.

Conventionally used Gauss/Seidel iterative method has several disadvantages. Since the matrices involved in the solution of statics equations have linear indeterminacies, direct solution with Gauss/Seidel method will not converge. To eliminate this instability the main diagonal of the matrix must be increased by a small percentage. This, consequently, will act as a low-pass filter on the computed results, losing fine details of short wave-length results. Another problem is, that the results are dependent on the initiation point of the computation. Computations starting with the source statics will differ from the ones starting with the receiver statics. Conjugate gradient method is a recursive solution of the whole set of equation, thus it will not be affected by the starting points. It is also immune from the instabilities of the equations, and the results are minimum distance to the starting values of the solutions, which are usually taken as a set of zero values.

A similar procedure using the least-mean-square approach with the conjugate gradient algorithm can be used to compute the source and receiver delays.

We have illustrated above how the 3-D refraction statics problem reduces to a formalism similar to the 2-D refraction statics solution. This formalism can be considered a unified method for solutions of 2-D and 3-D refraction statics.

SHORT WAVELENGTH SOLUTION

After the delay times and the slownesses are computed, their effects are removed from the original uphole corrected pick times. This will remove the relative elevation correction terms from the pick time values written as

$$t''(n, m) = T(n, m) - S(n) - R(m) - \sum_k [\sigma(k) \cdot \Delta(k)]. \quad (10)$$

Therefore $t''(n, m)$ now contains only the near surface weathering layer differential statics, which also contains the elevation statics in a residual manner, and possible uphole time errors. It is interesting to note that $t''(n, m)$ is basically the error term from the long wavelength solution. Since the long wavelength statics were computed from only the long wavelength smoothed arrival times and by setting the delay times equal for upward traveling (receiver) and the downward traveling (shot) waves, thus the resulting statics will be long wavelength statics. As above equation indicates that we subtract these long wavelength delay times (statics) from the original pick times to obtain the residual traveltimes with short wavelength disturbances. We decompose this traveltimes into shot and receiver surface (or short wavelength) statics. Note that we now separate the shot and the receiver statics. They are computed in a surface consistent manner by minimizing the equation

$$\varepsilon = \sum_n \sum_m [w(n, m) \cdot [t''(n, m) - s(n) - r(m)]]^2. \quad (11)$$

Here, again, we use weights in the same manner as the refraction statics computation to minimize the effects of erroneous picks. After all computations are completed, based on the overburden and refractor velocities, we compute the time it takes to go from the surface down to the refractor with given a overburden velocity and then back up to the datum level with the velocity of the consolidated deeper layers (Musgrave, 1967). Applying these corrections to data will bring the shots and receivers to the datum surface, remove the elevation, near surface weathered layer effects, and the effects of the slowly varying layer above the refracting layer.

2-D AND 3-D DATA EXAMPLES

Example 1

Our first example is a deep hole dynamite 2-D line. In this example, a total of 31 shots of 48-channel data with a length of 3 s and 2 ms sampling is used. The group interval is 220 ft (67 m), and the data is gathered at 6-fold. The raw stack with 110 ft common depth (CDP) trace interval without any statics application is shown in Figure 7a. We have used a weathering velocity of 3500 ft/s (1066 m/s) and subweathering velocity of 5500 ft/s (1670 m/s). The stack with conventional elevation statics is shown in Figure 7b. The first arrivals of the data was picked using a neural network first-break picking technique (Taner et al., 1988) and input to the refraction statics computation. The computed long and short period refraction statics were then applied to the data. Figures 7c and 7d show stacks with the short

or long period statics corrections, respectively. Figure 7e shows the stack with both the short and long period statics corrections. To demonstrate the effectiveness of the refraction statics, examples of shot records with and without refraction statics corrections are displayed in Figures 8a and 8b, respectively.

Example 2

The data in this 2-D example was acquired with a dynamite source in an end-on shooting pattern. It is a 48-channel recording, 3 s in length sampled at 4 ms. The group interval is 50 m and it is gathered at 24-fold. The weathering velocity is 1500 m/s and

the subweathering velocity is 2300 m/s. The brute stack section with elevation statics correction generated at 25 m CDP intervals is shown in Figure 9a. The events in the zone of interest around 2 s are discontinuous and apparently distorted by the statics problems. After the refraction statics corrections, the events are improved as shown in Figure 9b.

Example 3

This example shows a comparison of a 3-D data set with and without refraction statics application. Weathering velocity of 1300 m/s and a subweathering velocity of 2900 m/s is

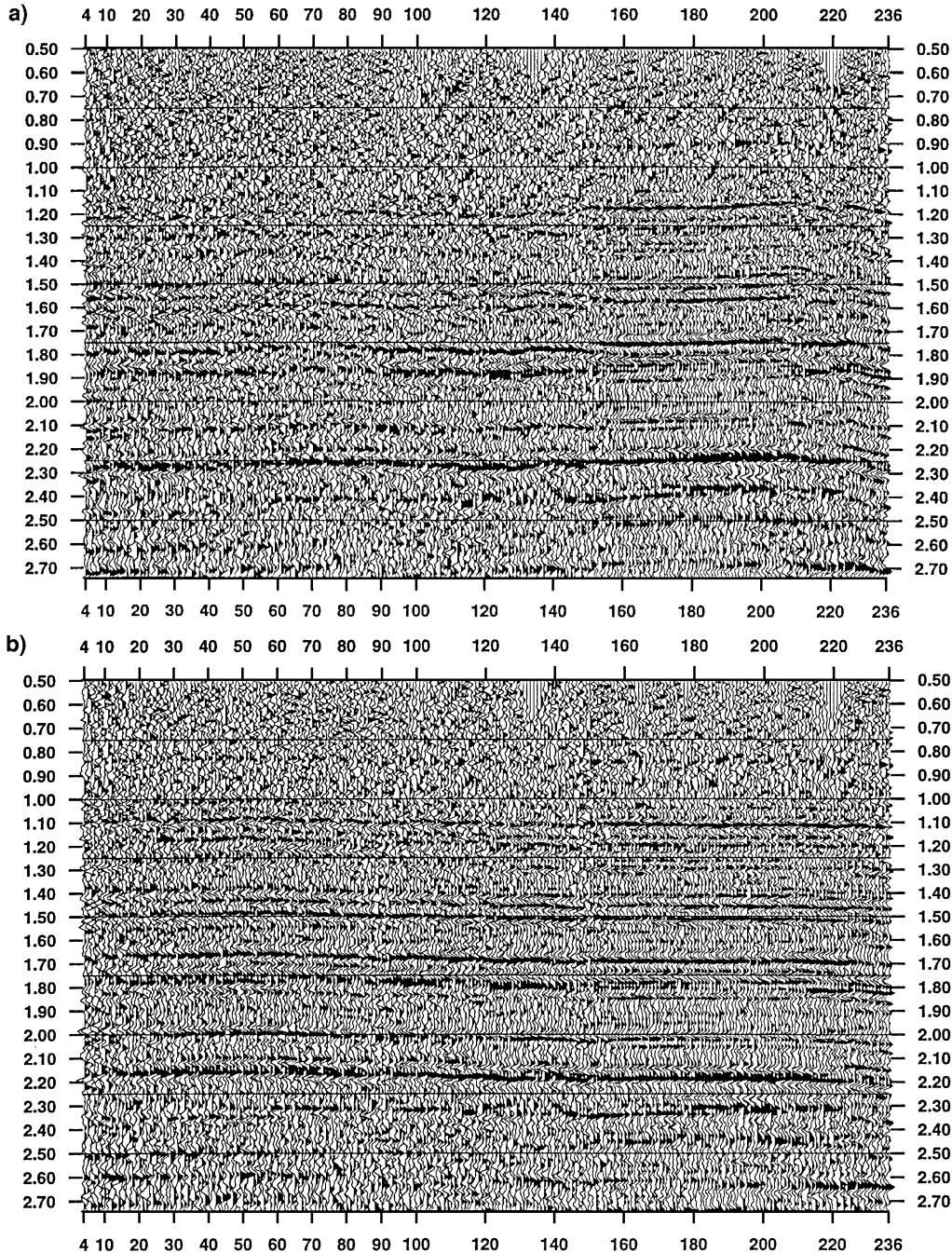


FIG. 7. (a) The raw stack without statics correction. (b) The stack section with elevation statics correction.

Unified Refraction Statics

used. The stacked trace interval is 50 m. The conventional brute stack section with elevation correction is shown in Figure 10a. The application of both statics (surface and refraction) (Figure 10b) successfully has removed the long and short wavelength statics in the data. The effectiveness can also be illustrated in the comparison of time slices at 940 and 944 ms shown in Figures 11a and 11b, respectively. To show effectiveness of convergence by this method, we computed the error statics associated with the long and short wavelength statics computation. Figure 12a shows the error distribution of long wavelength refraction statics and Figure 12b shows

the error distribution of short wavelength surface statics for this example. The concentration of errors at the smaller statics means that we have obtained a stable solution for both the long and short wavelength statics, and thus our model fits the data within the error ranges indicated on the graph.

CONCLUSION

We developed a near-surface model that is more suitable for surface and refraction statics computation. We have shown that the picked first-break traveltimes contain both refraction and near-surface weathered layer elevation and transmission

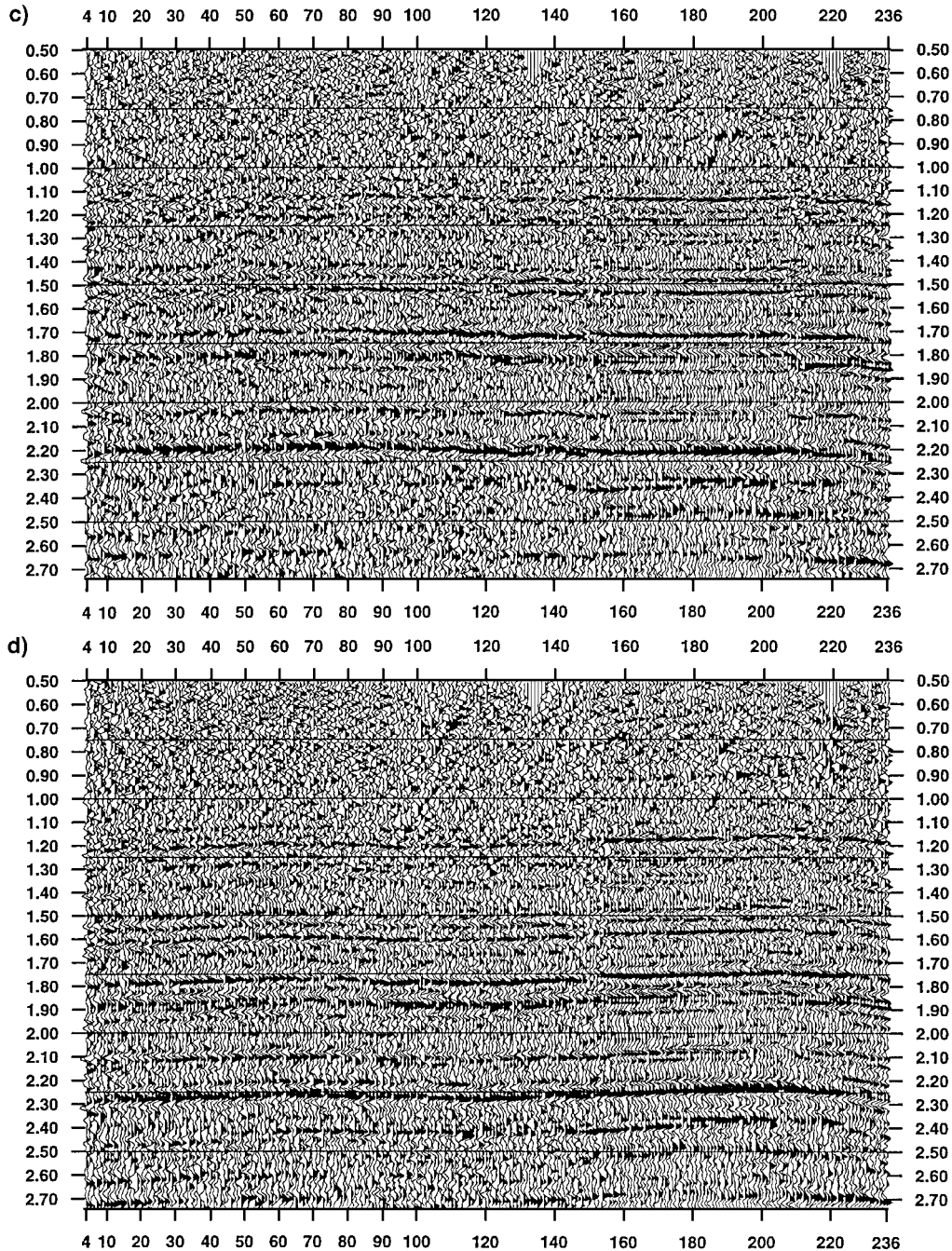


FIG. 7. (c) The stack section with long wavelength refraction statics correction. (d) The stack section with short wavelength refraction statics correction.

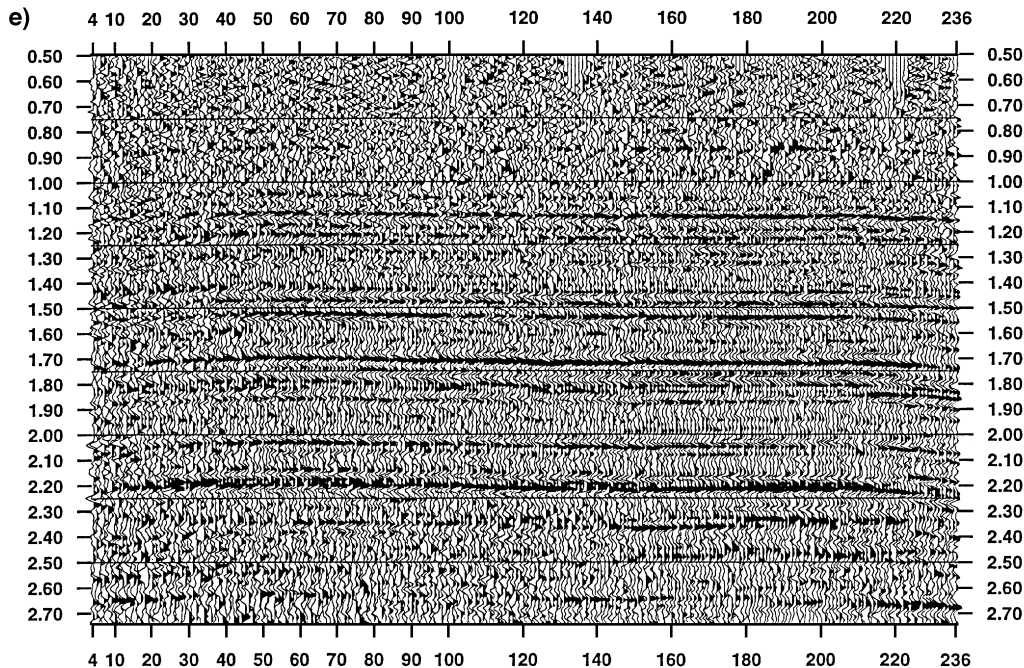


FIG. 7. (e) The stack section with both short and long wavelength refraction statics correction.

statics. This was supported by both the convergence of mathematical solutions and the appearance of the final stack sections. The ability to determine and apply static corrections for the near-surface weathering layer as well as the relative elevation statics reduces the residual reflection statics to residual levels, on the order of 1/4 of the wavelet width. With small residual statics, initial velocity estimates are more accurate, hence eliminating the velocity/statics interdependency dilemma. The method outlined in this paper is equally applicable to 2-D, 3-D and crooked or slalom lines. We have also shown that the method is robust and tolerates a certain amount of mispicks without ill-effects. We used the conjugate gradient solution without making any provisions for instabilities inherent in the statics equations.

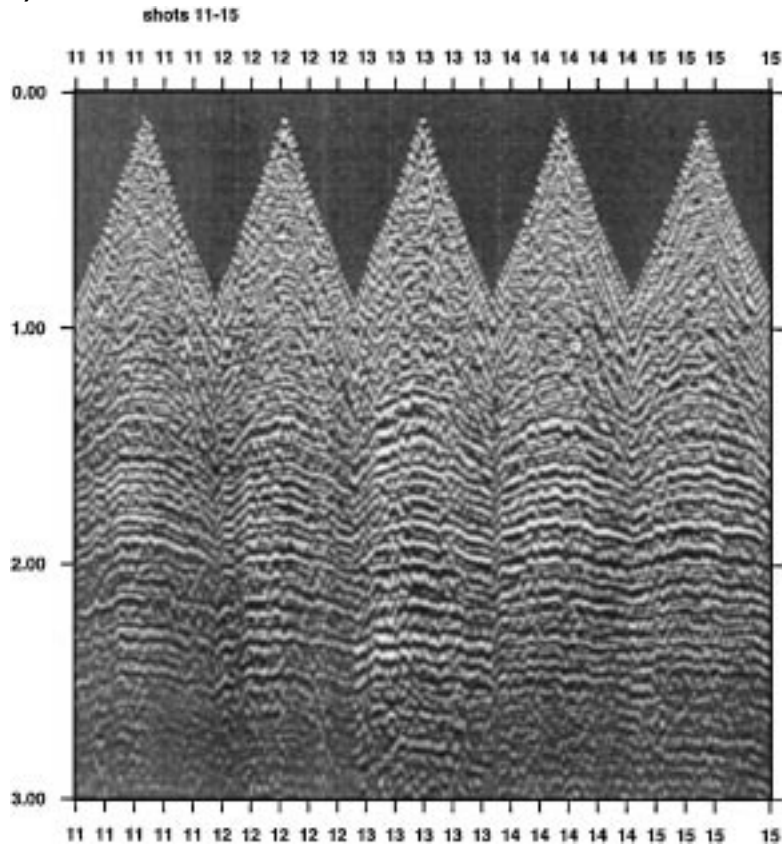
ACKNOWLEDGMENTS

We wish to thank Duane Dopkin and Chung-Chi Shih of CogniSeis for first-break picking and statics computation on the FOCUS system. We would also like to thank John Taner of Seismic Research Corporation for preparing this manuscript.

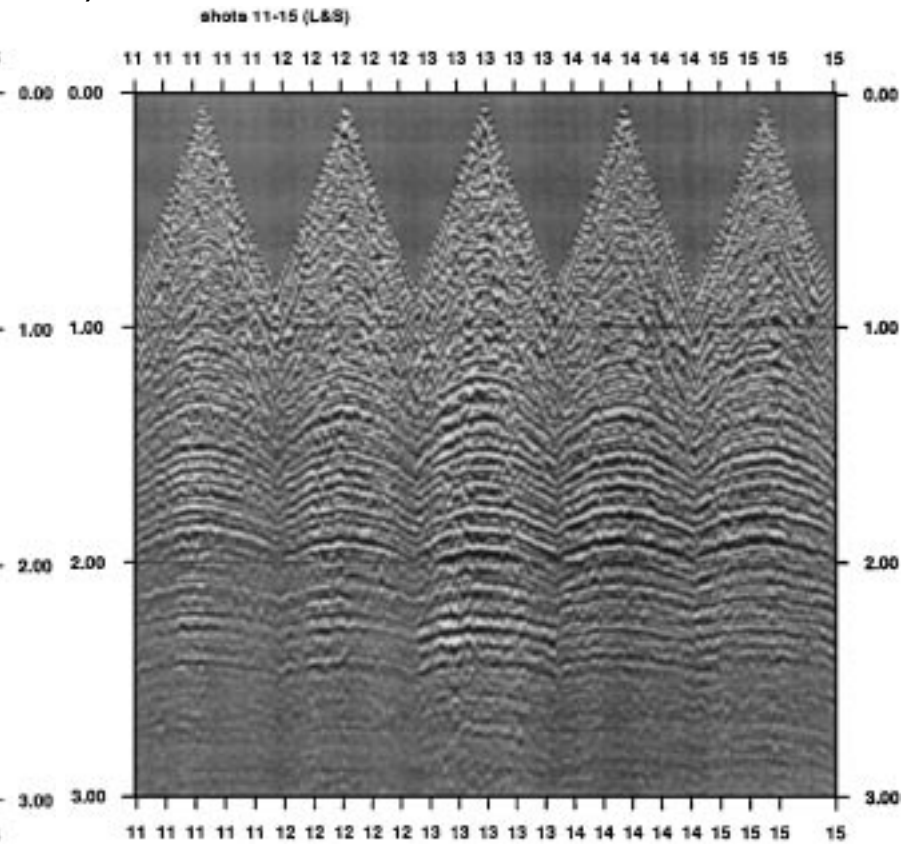
REFERENCES

- Ansel, E. A., 1930, Das impulsfeld der praktischen Seismik in graphischer Behandlung: Gerlands Ergänzungshefte für angewandte Geophysik, **1**, 117-136.
- Barry, K. M., 1967, Delay time and its application to refraction profile interpretation, in Musgrave, A. W., Seismic refraction prospecting: Soc. Expl. Geophysicists.
- Chon, Y. T., and Dillon, T. J., 1986, Tomographic mapping of the weathered layer; 56th Ann. Internat. Mtg. Soc. Expl. Geophys., Expanded Abstracts, 593-595.
- Chun, J. H., and Jacowitz, C. H., 1980, Automated statics estimation utilizing first-arrival refractions: Presented at the 50th Ann. Internat. Mtg., Soc. Expl. Geophys., held in Houston, TX.
- 1981, Weathering statics problem and first arrival time surfaces: Presented at the 51st Ann. Internat. Mtg. Soc. Expl. Geophys.
- Docherty, P., 1992, Solving for the thickness and velocity of the weathering layer using 2-D refraction tomography, Geophysics, **57**, 1397-1318.
- Farrell, R. C., and Euwema, R. N., 1984, Refraction statics: Proc. IEEE, **72**, 1316-1329.
- Gardner, L. M., 1939, An aerial plan of mapping subsurface structure by Refraction shooting: Geophysics, **4**, 274-259.
- Hagedoorn, J. G., 1959, The plus-minus method of interpreting seismic refraction sections: Geophys. Prosp., **7**, 158-182.
- Hampson, D., and Russell, B., 1984, First-break interpretation using generalized linear inversion: Presented at the 54th Ann. Internat. Mtg., Soc. Expl. Geophys., Expanded Abstracts, 532-534.
- Kirchheimer, F., 1988, A tomographic approach to 3-D refraction statics: Presented at the 50th meeting of Eur. Assoc. of Expl. Geophys.
- Koehler, F., and Taner, M. T., 1985, The use of the conjugate-gradient algorithm in the computation of predictive deconvolution operators: Geophysics, **50**, 2752-2558.
- Musgrave, A. W. ed. 1967, Seismic refraction prospecting: Soc. Expl. Geophys.
- Palmer, D., 1980, The generalized reciprocal method of seismic refraction interpretation: Soc. Expl. Geophys.
- Robinson, E. A., and Osman, M. O., 1996, Seismic Source Signature estimation and measurements, reprint series No. 18: Soc. Expl. Geophys. Geophysics.
- Schneider, W. A., and Kuo, S., 1985, Refraction modeling for static corrections: Ann. Internat. Mtg., Soc. Expl. Geophys., Expanded Abstracts, 295-299.
- Sheriff, R. E., 1991, Encyclopedic dictionary of exploration geophysics: Soc. Expl. Geophys.
- Taner, M. T., 1988, The use of supervised learning in first-break picking; in Bielanski, E. Ed., Proc. Symp. Geophys. Soc. Tulsa.
- Taner, M. T., Lu, L., and Baysal, E., 1988, Unified method for 2-D and 3-D refraction statics with first-break picking by supervised learning; 58th Ann. Internat. Mtg., Soc. Expl. Geophys., Expanded Abstracts, 772-774.
- Taner, M. T., Matsuoka, T., Baysal, E., Lu, L., and Yilmaz, O., 1992, Imaging with refractive seismic waves: 62nd Ann. International Mtg., Soc. Expl. Geophys., Expanded Abstracts, 1132-1135.
- Thornburgh, H. R., 1930, Wavefront diagrams in seismic interpretation: AAPG Bull., **14**, 185-200.
- Veezhinathan, J., and Wagner, D., 1990, A neural network approach to first-break picking: Proc. Internat. Joint Conf. on Neural Networks, **1**, 235-240.
- Veezhinathan, J., Wagner, D., and Ehlers, J., 1991, First-break picking using a neural network, in Aminzadeh, F. and Simaan, M., Eds., Expert systems in exploration, Geophysical development No. 3: Soc. Expl. Geophys. Conference on Neural Networks, San Diego CA.
- Wang, R. J., and Treitel, S., 1973, The Determination of digital Wiener filters by means of gradient methods: Geophysics, **38**, 310-326.

a)



b)



Unified Refraction Statics

FIG. 8. (a) The raw shot records. (b) The shot records after refraction statics correction.

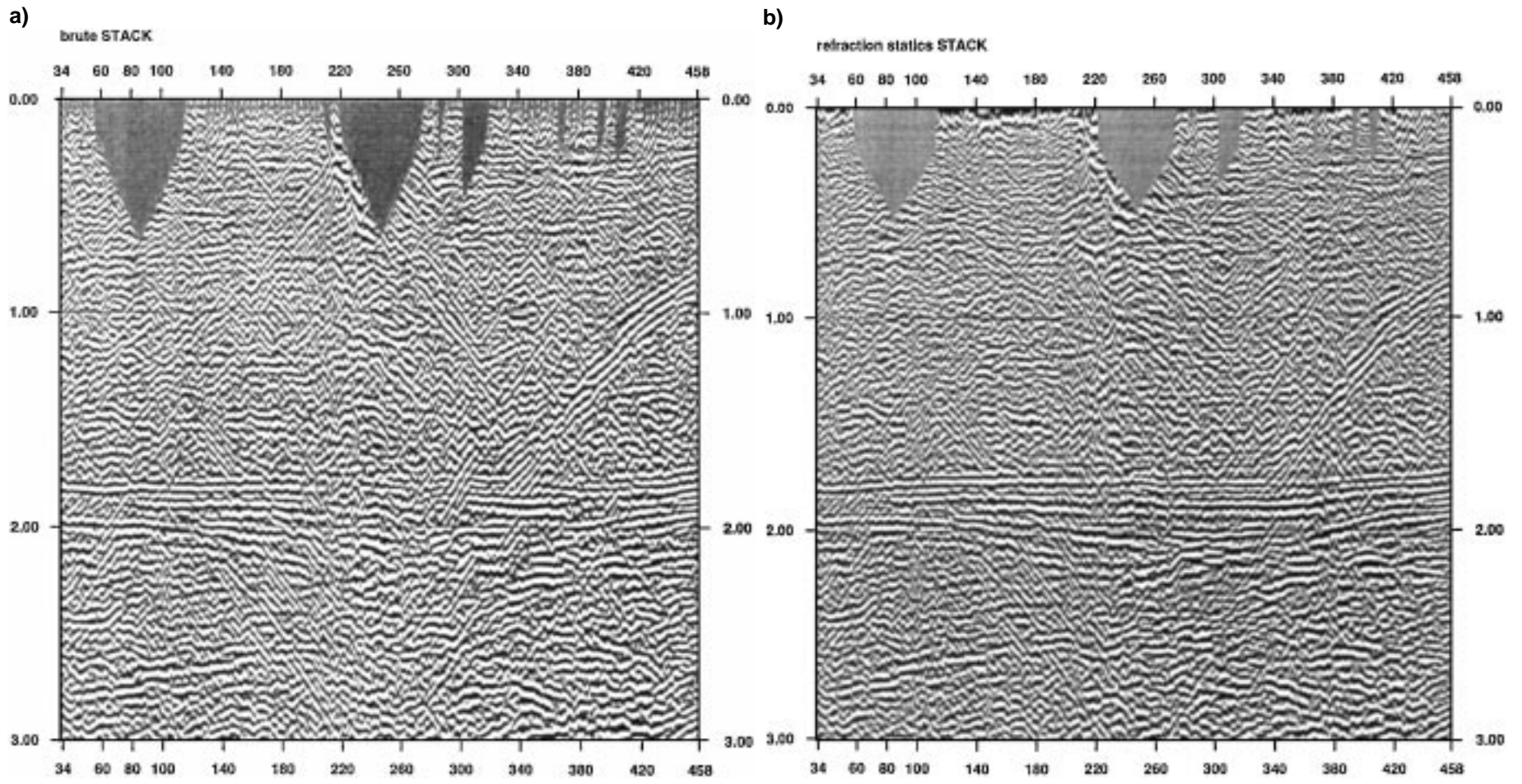


FIG. 9. (a) The brute stack section. (b) The section with refraction statics correction.

Unified Refraction Statics

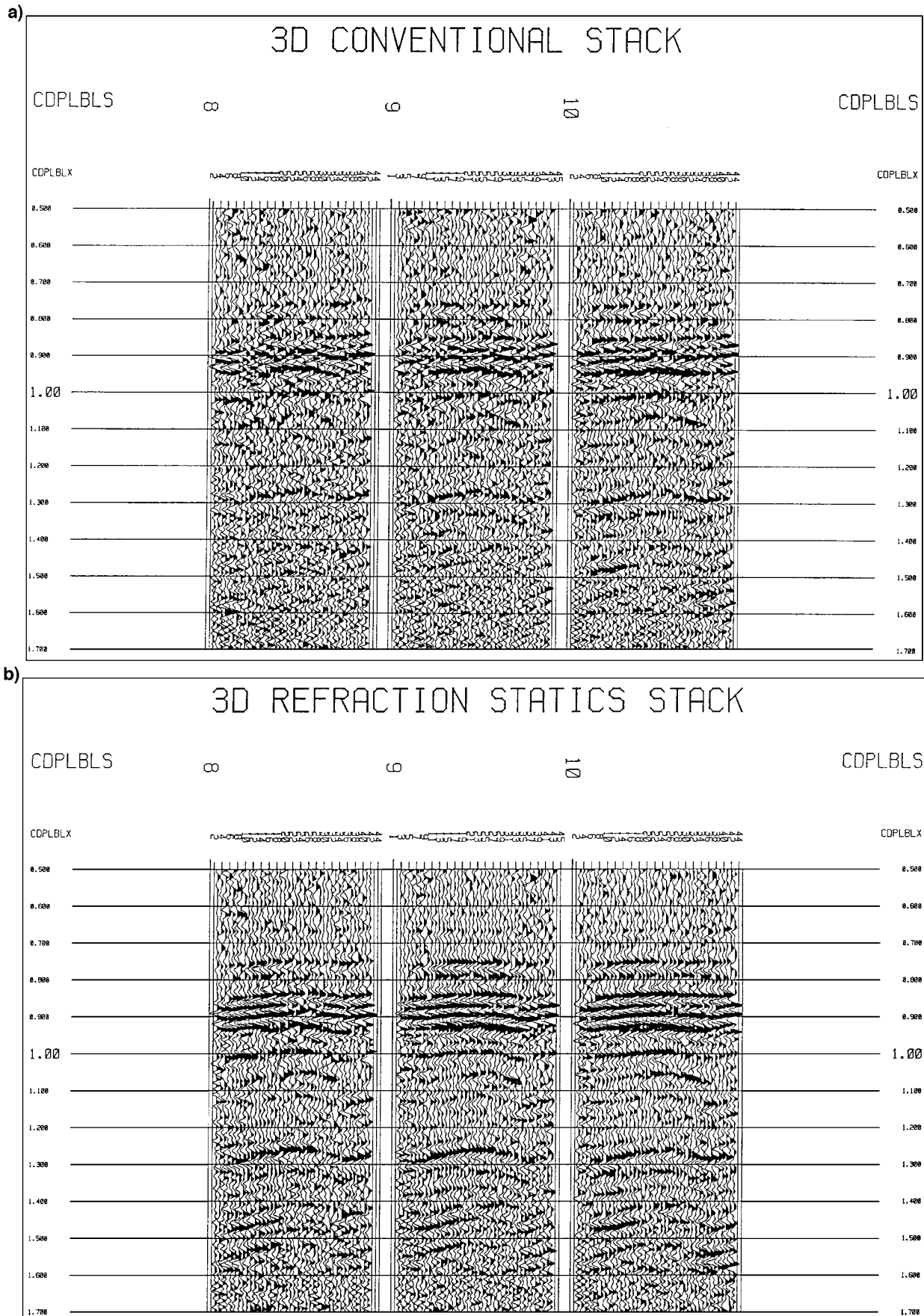


FIG. 10. (a) An inline section of a 3-D brute stack. (b) The inline section after refraction statics correction.

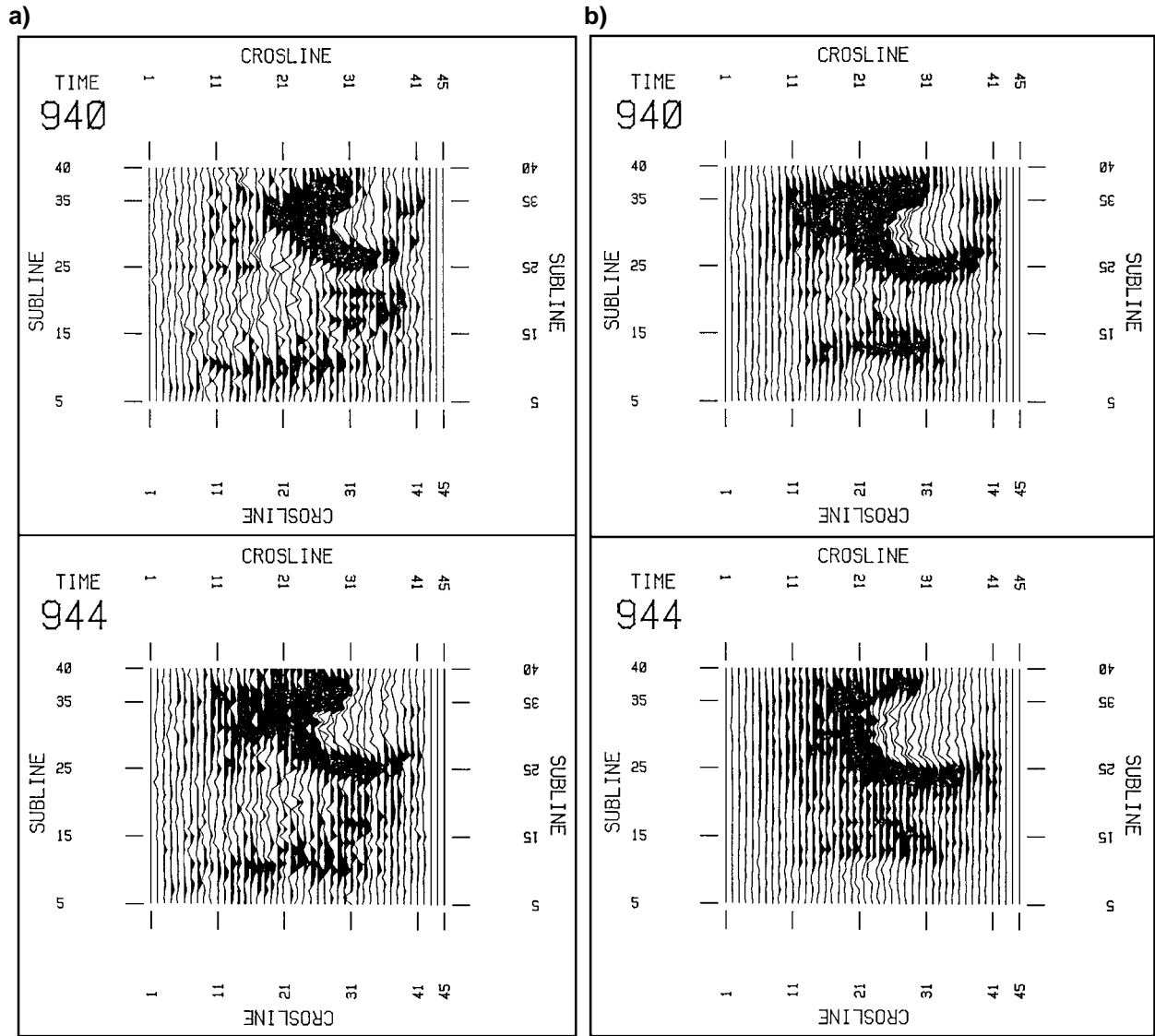


FIG. 11. (a) Time slices of the 3-D brute stack. (b) The time slices after refraction statics correction.

Unified Refraction Statics

a) COMPUTATION ERROR STATISTICS

STANDARD DEVIATION = 10.84
 TOTAL NUMBER OF PICKS = 14829

ERROR (MS)	POPULATION	PERCENT	DISTRIBUTION
-100.0	3.	0	
-96.0	1.	0	
-92.0	3.	0	
-88.0	0.	0	
-84.0	1.	0	
-80.0	3.	0	
-76.0	1.	0	
-72.0	1.	0	
-68.0	1.	0	
-64.0	1.	0	
-60.0	4.	0	
-56.0	6.	0	
-52.0	6.	0	
-48.0	5.	0	
-44.0	11.	0	
-40.0	7.	0	
-36.0	4.	0	
-32.0	8.	0	
-28.0	15.	0	
-24.0	41.	0	*
-20.0	85.	1	*
-16.0	239.	2	***
-12.0	584.	4	*****
-8.0	1455.	10	*****
-4.0	2724.	18	*****
0.0	3061.	21	*****
4.0	2651.	18	*****
8.0	1686.	11	*****
12.0	1064.	7	*****
16.0	601.	4	*****
20.0	281.	2	****
24.0	144.	1	**
28.0	62.	0	*
32.0	23.	0	*
36.0	32.	0	*
40.0	11.	0	
44.0	2.	0	
48.0	0.	0	
52.0	1.	0	
56.0	0.	0	
60.0	0.	0	
64.0	0.	0	
68.0	0.	0	
72.0	0.	0	
76.0	0.	0	
80.0	0.	0	
84.0	0.	0	
88.0	0.	0	
92.0	0.	0	
96.0	0.	0	
100.0	1.	0	

FIG. 12. (a) Error distribution for long wavelength refraction statics computation. (b) Error distribution for short-wavelength refraction statics computation.

b) COMPUTATION ERROR STATISTICS

STANDARD DEVIATION	=	9.14	
TOTAL NUMBER OF PICKS	=	14829	
ERROR (MS)	POPULATION	PERCENT	DISTRIBUTION
-100.0	4.	0	
-96.0	2.	0	
-92.0	2.	0	
-88.0	0.	0	
-84.0	3.	0	
-80.0	1.	0	
-76.0	0.	0	
-72.0	2.	0	
-68.0	2.	0	
-64.0	1.	0	
-60.0	5.	0	
-56.0	7.	0	
-52.0	9.	0	
-48.0	8.	0	
-44.0	8.	0	
-40.0	5.	0	
-36.0	6.	0	
-32.0	8.	0	
-28.0	7.	0	
-24.0	26.	0	
-20.0	59.	0	*
-16.0	92.	1	*
-12.0	269.	2	**
-8.0	852.	6	*****
-4.0	3154.	21	*****
0.0	5191.	35	*****
4.0	2970.	20	*****
8.0	1240.	8	*****
12.0	467.	3	****
16.0	234.	2	**
20.0	96.	1	*
24.0	34.	0	*
28.0	30.	0	
32.0	24.	0	
36.0	7.	0	
40.0	2.	0	
44.0	1.	0	
48.0	0.	0	
52.0	0.	0	
56.0	0.	0	
60.0	0.	0	
64.0	0.	0	
68.0	0.	0	
72.0	0.	0	
76.0	0.	0	
80.0	0.	0	
84.0	0.	0	
88.0	0.	0	
92.0	0.	0	
96.0	0.	0	
100.0	1.	0	

FIG. 12. (Continued.)